Available online at www.sciencedirect.com
ScienceDirect
Journal of Solid State Chemistry 180 (2007) 2110–2115
JOURNAL OF SOLID STATE CHEMISTRY
www.elsevier.com/locate/jssc

$Na(H_3NCH_2CH_2NH_3)_{0.5}[Co(C_2O_4)(HPO_4)]$: A novel phosphoxalate open-framework compound incorporating both an alkali cation and an organic template in the structural tunnels

Tao Huang, Britt A. Vanchura, Yongkui Shan, Songping D. Huang*

Department of Chemistry, Kent State University, Kent, OH 44242, USA

Received 18 January 2007; received in revised form 7 May 2007; accepted 8 May 2007
Available online 18 May 2007

Abstract

The first open-framework metal phosphoxalate compound containing both an organic and an inorganic template in the same structure is reported. $Na(H_3N^+CH_2CH_2N^+H_3)_{0.5}[Co(C_2O_4)(HPO_4)]$ (**1**) was synthesized hydrothermally via a direct metathesis reaction using the sodium salts of oxalate and phosphate in the presence of cobalt chloride and ethylenediamine dihydrochloride. The structure of **1** consists of a 3D framework built from the $[Co(C_2O_4)]_n$ layers connected by HPO_4^{2-} group bridging two different cobalt centers between the adjacent layers. A major and a minor structural tunnels are created and occupied by the Na^+ and $H_3N^+CH_2CH_2NH_3^{2+}$ ions, respectively, in the same structure. Single-crystal X-ray crystallographic data for **1** are: monoclinic, $P2_1/c$, $a = 5.8189(6)$, $b = 10.235(1)$, $c = 13.066(1)$ Å, $\beta = 96.671(2)^\circ$, $Z = 4$, $V = 772.9(1)$ Å^3, $R = 3.95\%$ and $R_w = 6.37\%$.

Keywords: Cobalt phosphoxalate; Cobalt oxalate; Cobalt phosphate; Organic–inorganic hybrid compound; Open-framework

1. Introduction

Open-framework metal phosphate compounds with diverse structural chemistry and many potential applications have garnered great attention recently [1–5]. Those gaining quite a bit of this attention are organic–inorganic hybrids. The use of organic molecules in skeletons of inorganic open-framework structures has been shown to be effective in producing diverse structures. This method is now being used most notably with the oxalate as a co-ligand and amines as templates in metal phosphates after several research groups have been able to synthesize novel phosphoxalate materials with channels similar to those found in zeolites and aluminophosphates. The added flexibility that the oxalate group brings to the inorganic framework is envisioned for creating interesting properties for these structures. Thus far, a large number of such hybrid organic–inorganic framework structures have been derived from either the main group metals or the transition elements include Al [6–9], Co [10], Fe [11–21], Ga [22–26], In [27–30], Mn [31–35], Mo [36], Sn [37], V [38–41] and Zn [42,43]. However, all of the known compounds in this class have been synthesized by the use of an organic amine such as ethylenediamine, piperazine or other mono- or di-amines as the base to deprotonate both oxalic and phosphoric acids in situ to meet the pre-requisite for metal complexation and framework assembly under hydrothermal conditions. Once protonated, the amine molecule can act as the charge compensator as well as the structure-directing template through its geometric imprinting and/or H-bonding with the framework oxygen atoms, and thus being self-included in a cavity of the structure. Although synthetically straightforward and convenient, this approach limits the type of template molecules that can be incorporated into such open-framework structures to those with considerable Brønsted basicity. Up to now, there have been only two examples where attempts are made to introduce the organic template molecules using their quaternary salt form (i.e., $(CH_3)_4NBr$ and $(C_4H_9)_4NBCl$)

*Corresponding author. Fax: +1 330 672 3816.
E-mail address: shuang1@kent.edu (S.D. Huang).

0022-4596/$ - see front matter © 2007 Elsevier Inc. All rights reserved.
doi:10.1016/j.jssc.2007.05.006

[14,23]. However, in both cases, the resultant structures fail to encapsulate the intended templates. In light of our interest in incorporating optically, electrochemically or magnetically active cationic organic, organometallic and metal-organic molecules (e.g., viologens, tris-bipyridyl-ruthenium and metalloceniums) into phosphoxalate structures, a non acid–base reaction route to such open-framework materials may prove to be valuable for expanding the includible template molecules into general cationic species of organic, organometallic and metal-organic nature. In this paper, we report on the successful synthesis of a novel metal phosphoxalate compound, $Na(H_3N^+CH_2CH_2N^+H_3)_{0.5}[Co(C_2O_4)(HPO_4)]$ (**1**), via a direct metathesis reaction between $H_3NCH_2CH_2NH_3Cl_2$, $Na_2C_2O_4$ and Na_2HPO_4 in the presence of $CoCl_2 \cdot 6H_2O$ under hydrothermal conditions. This approach may open up a new avenue for incorporating other non-amine-based cationic templates into this class of compounds. Furthermore, due to the presence of both the sodium cation and the diprotonated ethylenediamine molecule in two different tunnels created in the same structure, **1** is the first hosphoxalate open-framework compound containing both inorganic and organic cations as the structure-directing templates.

2. Experimental

2.1. Synthesis

All reagents were purchased from Fischer Scientific International Inc. and used without further purification. Compound **1** was synthesized from a reaction mixture with the composition 1.0 mmol $H_3NCH_2CH_2NH_3Cl_2$:2.0 mmol $CoCl_2 \cdot 6H_2O$:2.0 mmol $Na_2C_2O_4$:2.0 mmol Na_2HPO_4. Ethylenediamine dihydrochloride (0.798 g), cobalt chloride hexahydrate (2.85 g) and sodium oxalate (1.61 g) were first added to a 21-mL Teflon-lined autoclave cup along with 5 mL of water and stirred to result in a dark pink suspension. Dibasic sodium phosphate (1.70 g) was then added with stirring, and the suspension was sealed in the autoclave. Reaction and crystallization took place under autogeneous pressure at 160 °C for 1 week to afford purple-red crystals of **1** in essentially quantitative yield. $C_3H_6CoNNaO_8P$ (FW = 296.98): calcd.: C 12.12, H 2.02, N 4.71; found: C 12.07, H 1.98, N 4.62. The phase purity of the product was confirmed by a peak-to-peak match between the experimentally observed X-ray powder diffraction pattern (XRD) of **1** and the simulated powder pattern using single-crystal structure data (see Fig. 1 of the Supplementary Materials).

2.2. Characterization

The elemental analyses were conducted on a Perkin-Elmer 240C element analyzer. The X-ray powder diffraction patterns were obtained from a palletized bulk sample on a Bruker D500 powder X-ray diffractometer. The thermal analysis was conducted on a TGA 2950 high-resolution thermogravimetric analyzer (New Castle, DE, USA) in air with a heating rate of 5 °C/min. Solid-state diffuse reflectance spectra were measured with a Shimadzu UV-2401PC spectrophotometer equipped with an ISR-2200 integrating sphere attachment in the wavelength range of 250–900 nm using $BaSO_4$ powder as a reflective standard (100% reflectance). The Kubelka–Munk function was applied to convert the reflectance data into *pseudo* absorbance.

2.3. Structure determination

A suitable needle-shaped purple-red single crystal with dimensions $0.22 \times 0.08 \times 0.04$ mm was selected under a polarizing microscope. Preliminary screening and intensity data collection was performed on a Bruker SMART-CCD diffractometer equipped with a normal focus, 2.4 kW sealed tube X-ray source (Mo$K\alpha$ radiation, $\lambda = 0.71073$ Å) operating at 50 kV and 40 mA. A hemisphere of intensity data was collected at room temperature in 1321 frames with exposure time of 10 s per frame in the θ range of 1.57–27.06°.

The structure was solved by direct methods and refined using the teXsan package [44]. An empirical absorption correction based on symmetry equivalent reflections was applied using the SADABS program. All of the non-hydrogen atoms were refined anisotropically. Hydrogen atoms were added according to theoretical models. The crystallographic data and structure determination parameters for compound **1** are summarized in Table 1. The fractional atomic positions and the equivalent displacement parameters are given in Table 2. Selected bond distances for **1** are reported in Table 3.

3. Results and discussion

3.1. Synthetic strategy

Up to now, the only established route to open-framework phosphoxalates makes use of the Brønsted acid

Table 1
Crystal data and structure refinement parameters for $Na(H_3N^+CH_2CH_2N^+H_3)_{0.5}[Co(C_2O_4)(HPO_4)]$

Empirical formula	$C_3H_6CoNNaO_8P$
Formula weight	296.98
Temperature (K)	296
Crystal system	Monoclinic
Space group	$P2_1/c$
Unit cell dimensions	
	$a = 5.8189(6)$ Å, $\alpha = 90°$
	$b = 10.235(1)$ Å, $\beta = 96.671(2)°$
	$c = 13.066(1)$ Å, $\gamma = 90°$
Z, V (Å^3)	4, 772.9(1)
Density (calcd., g/cm^3)	2.55
Abs. coeff. (mm^{-1})	2.513
No. of reflns. collected	4132
No. of independent reflns.	1636
Data/restraints/params	1184/0/137
GOF	0.995
Final R indices [$I > 2\sigma(I)$]	$R = 3.95\%$ and $R_w = 6.37\%$
Largest peak and hole (e/Å^3)	0.67 and −0.37

Table 2
Atomic coordinates and thermal parameters (Å^2) for $Na(H_3N^+CH_2CH_2N^+H_3)_{0.5}[Co(C_2O_4)(HPO_4)]$

Atom	x	y	z	U_{eq}[a]
Na(1)	0.8877(2)	0.0523(1)	0.3702(1)	0.0177(4)
Co(1)	0.35498(7)	0.25171(4)	0.23987(3)	0.0097(1)
P(1)	0.3892(1)	0.20321(8)	0.49267(7)	0.0109(2)
O(1)	0.3773(4)	0.2909(2)	0.5865(2)	0.0153(6)
O(2)	0.6488(4)	0.1513(2)	0.4984(2)	0.0187(6)
O(3)	0.3494(4)	0.2873(2)	0.3954(2)	0.0160(6)
O(4)	0.2285(4)	0.0861(2)	0.4895(2)	0.0156(6)
O(5)	0.2065(4)	0.0664(2)	0.2540(2)	0.0124(6)
O(6)	0.4670(4)	0.4490(2)	0.2264(2)	0.0137(6)
O(7)	0.7307(4)	0.2299(2)	0.2611(2)	0.0140(6)
O(8)	1.0308(3)	0.3465(2)	0.2160(2)	0.0154(6)
N(1)	0.7891(5)	0.0414(3)	0.0936(2)	0.0165(8)
C(1)	0.8277(5)	0.3334(3)	0.2380(2)	0.0108(8)
C(2)	0.6828(5)	0.4605(3)	0.2359(2)	0.0097(8)
C(3)	0.9008(6)	0.0479(3)	−0.0026(3)	0.0168(9)

[a] U_{eq} is defined as one-third of the trace of the orthogonalized U_{ij} tensor.

Table 3
Selected bond lengths (Å) for $Na(H_3N^+CH_2CH_2N^+H_3)_{0.5}[Co(C_2O_4)(HPO_4)]$

Co(1)–O(1)	2.070(2)	Co(1)–O(3)	2.069(2)
Co(1)–O(5)	2.101(2)	Co(1)–O(6)	2.135(2)
Co(1)–O(7)	2.183(2)	Co(1)–O(8)	2.112(2)
P(1)–O(1)	1.528(2)	P(1)–O(2)	1.594(2)
P(1)–O(3)	1.530(2)	P(1)–O(4)	1.518(2)
O(5)–C(2)	1.260(4)	O(6)–C(2)	1.253(4)
O(7)–C(1)	1.253(4)	O(8)–C(1)	1.256(4)
Na(1)–O(2)	2.512(3)	Na(1)–O(4)	2.401(2)
Na(1)–O(4)	2.472(3)	Na(1)–O(5)	2.534(2)
Na(1)–O(6)	2.523(2)	Na(1)–O(7)	2.422(2)
Na(1)–O(8)	2.460(2)		
H(1)···O(1)	1.95	H(2)···O(3)	1.82
H(3)···O(5)	2.39	H(3)···O(7)	2.60

properties of both oxalic and phosphoric acids. The typical synthesis begins with addition of an organic amine to the mixture of the two acids and a metal salt in a proper ratio. Because the resultant frameworks invariably bear a negative charge and the protonated amine molecules are the only available cations in the synthesis, structure assembly directed by the template molecules is usually ensured by the electroneutrality requirements of the overall structure. Such simple method has proven to be not only straightforward but also effective, as all of the open-framework phosphoxalate compounds known to date have been prepared via this route. However, if non-amine-based cationic molecules such as methylviologen, Cp_2Fe^+ and $Ru(2,2'\text{-bipy})_3^{2+}$ are to be used as the template, a different synthetic method needs to be developed. We carried out a simple direct metathesis reaction between $H_3NCH_2CH_2NH_3Cl_2$, $Na_2C_2O_4$, Na_2HPO_4 and $CoCl_2\cdot 6H_2O$ under hydrothermal conditions at 160 °C, and successfully obtained compound **1**, the first open-framework metal phosphoxalate compound synthesized by the new method. The mass balanced equation for the synthesis of **1** can therefore be given as follows:

$$0.5H_3NCH_2CH_2NH_3Cl_2 + CoCl_2\cdot 6H_2O + Na_2C_2O_4 + Na_2HPO_4 \rightarrow Na(H_3NCH_2CH_2NH_3)_{0.5}[Co(C_2O_4)(HPO_4)] + 3NaCl + 6H_2O$$

Interestingly, when the same reactants were refluxed in 200 mL water for 6 days, the product obtained after isolation and washing with water and ethanol was identified by X-ray powder diffraction (XRD) to be $Co_3(PO_4)_2$. This indicates that the solution reaction favors the formation of the thermodynamically more stable binary phase, while the hydrothermal technique can stabilize the kinetically controlled compound **1**. On the other hand, when the Na^+ ion is replaced with K^+, Rb^+ or Cs^+ ion, the analogous compound $A(H_3NCH_2CH_2NH_3)_{0.5}[Co(C_2O_4)(HPO_4)]$ ($A = K^+$, Rb^+, Cs^+) was not formed. Instead, the only product isolated from these reactions was $(H_3NCH_2CH_2NH_3)_{0.5}[CoPO_4]$, a known cobalt phosphate open-framework compound containing no alkali metal ions in the structure [45]. This experiment suggests that the Na^+ ion can act as a structure-directing template as well as a charge compensator in the system.

3.2. Structure description

The asymmetric unit in **1** contains a Na^+ cation, half a $H_3N^+CH_2CH_2N^+H_3$ dication, a $C_2O_4^{2-}$ anion, a HPO_4^{2-} anion and a Co^{2+} ion. All of these atoms are situated on general positions. When the structure is expanded by the symmetry operations, the $[Co(C_2O_4)]$ fragment of the structure forms an infinite 2D sheet as shown in Fig. 1. Each cobalt center is surrounded by four oxygen atoms from three different $C_2O_4^{2-}$ anions. The O atoms in each $C_2O_4^{2-}$ anion can be divided into chelating and doubly bridging. The HPO_4^{2-} anion acts as a bidentate ligand that coordinates to two different metal centers in the adjacent layers, thus leading to the formation of a 3D network while completing the octahedral coordination for cobalt (see Fig. 2). The Co–O bond distances range from 2.069(2) to 2.183(2) Å, and the O–Co–O bond angles vary between 85.83(9)° and 108.22(8)°, and between 158.40(8)° and 173.40(8)°. All of these and other bond angles and bond distances in **1** are found to be comparable to those found in $[N_2C_4H_{12}]_{0.5}[Co_2(HPO_4)(C_2O_4)_{1.5}]$ [10]. The latter is thus far the only reported cobalt phosphoxalate compound in the literature. The H atom on this phosphate ligand could not be directly located from the difference Fourier maps. Its presence is implied by electroneutrality of the compound and the presence of the cobalt ion in the +2 oxidation state confirmed by its electronic spectrum (vide infra). On the whole, **1** has an open-framework structure with the $H_3N^+CH_2CH_2N^+H_3$ dication occupying a major channel and the Na^+ ion encapsulated in a minor channel. The Na^+ ion is nested in a distorted pentagonal bipyramidal pocket, interacting with seven oxygen atoms in a distance ranging from to 2.401(2) to 2.534(2) Å. Fig. 3 is a ball-and-stick representation of **1** as viewed down the

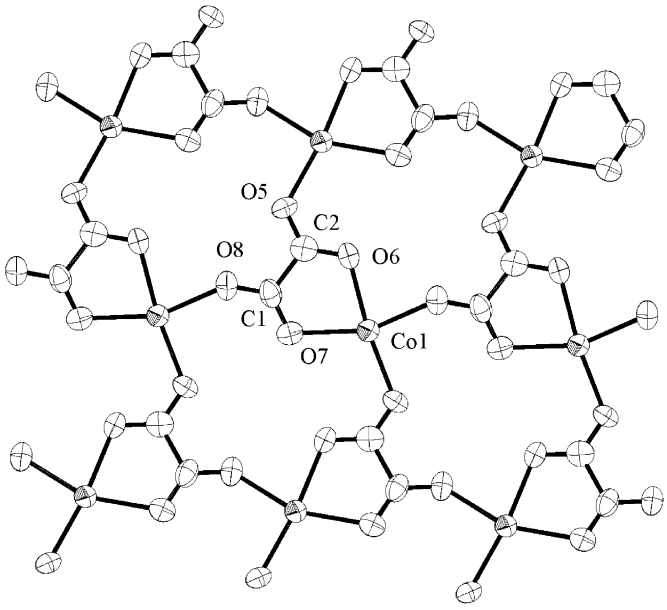

Fig. 1. The ORTEP representation of a 2D $[Co(C_2O_4)]$ sheet.

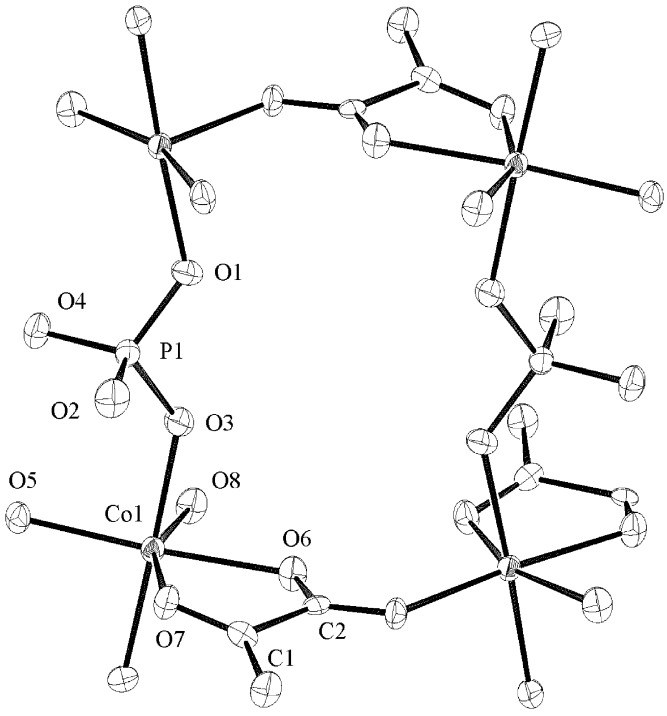

Fig. 2. A cutout view of **1** showing the HPO_4^{2-} coordination between two adjacent $[Co(C_2O_4)]$ layers.

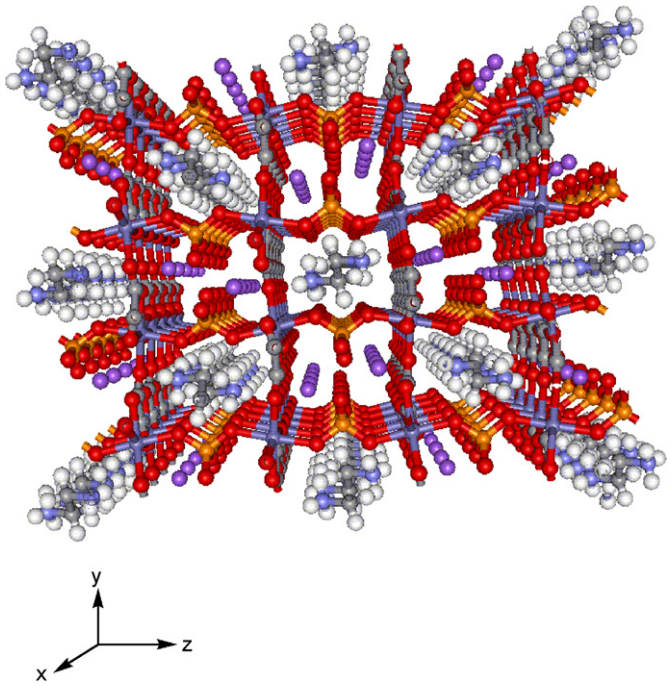

Fig. 3. The ball-and-stick representation of the 3D open-framework structure of **1** as viewed down the *a*-axis.

a-axis. There are extensive H-bonding interactions between the protonated amine groups and the O atoms from both the oxalate and the phosphate ligands. Of the three terminal amine H atoms, two of them each form a strong H-bond with two different O atoms from the phosphate ligand at 1.82 and 1.95 Å (see Table 3). The bond angles around these two H atoms are 168° and 175°. The third H atom concurrently forms moderate H-bonds with two different O atoms from the oxalate ligand at 2.85 and 2.60 with bond angles around 117°.

3.3. Diffuse reflectance optical spectrum

The solid-state diffuse reflectance spectrum of **1** measured at room temperature revealed the characteristic d–d transition absorption peak of the cobalt ion centered around 485 nm with a shoulder appearing at about 464 nm as shown in Fig. 4. These may be attributable to the spin-allowed electronic transitions, $^4T_{1g}(P) \leftarrow {}^4T_{1g}(F)$ and $^4T_{1g}(P) \leftarrow {}^4A_{2g}(F)$, typically found for the high-spin Co^{2+} ion in an octahedral environment. In addition to the discrete energy levels such as those revealed by the electronic transitions, other more extensive orbital overlap in **1** also results in the formation of bands because of the extended solid-state bonding in the structure. This assessment is based on the observation of an absorption edge identifiable below ~384 nm in the optical spectrum, indicating that the compound has an optical bandgap of ca. 3.2 eV. This value, comparable to that of bulk anatase TiO_2 of ca. 3.15 eV, places **1** as a borderline wide-bandgap semiconductor. Because of such large bandgap, very few electrons can be thermally promoted to the conduction band at temperatures below the thermal decomposition (vide infra), **1** is expected to show insulating properties.

3.4. Magnetic properties

Magnetic susceptibility measurements of **1** carried out using a SQUID in the temperature range of 5–300 K at the

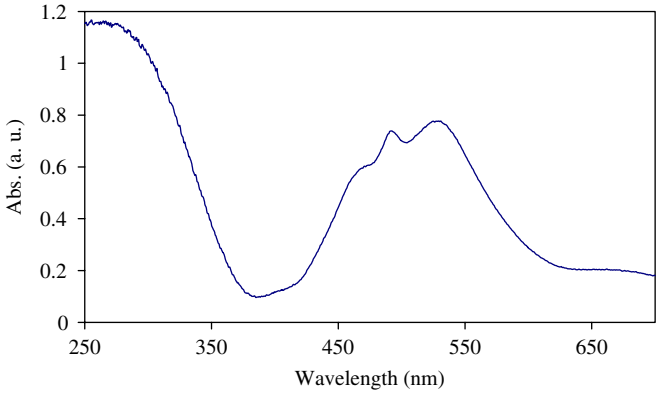

Fig. 4. The solid-state diffuse reflectance spectrum of **1** measured at room temperature.

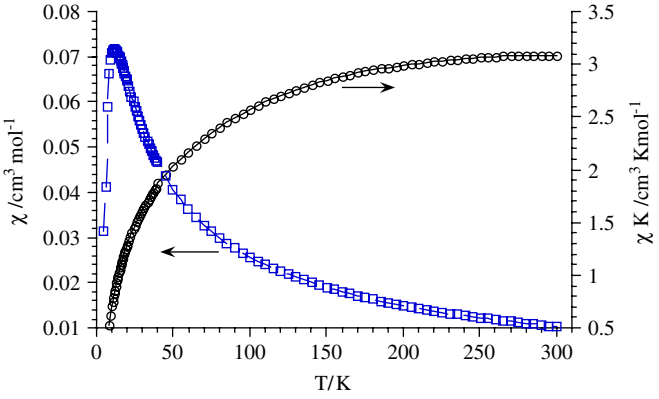

Fig. 5. χ and χT versus temperature plots for **1**.

field strength of 1000 G showed long-range order. Fig. 5 is the plots of both χ and the χT product versus temperature. The molar susceptibility χ first rises with decreasing temperature exhibits paramagnetic behavior in the high-temperature region (above 10 K) and antiferromagnetic interactions at the temperatures below 10 K. The fitting of high-temperature (above 10 K) data with the Currie–Weiss law yielded $\theta_p = -34.8$ K and $C = 3.48\,cm^3\,K/mol$. The measured effective magnetic moment of 4.97 μ_B at 300 K is slightly higher than the spin-only value of 4.90 μ_B. These results suggest that **1** contains the high-spin octahedral Co^{2+} ion $\left(t_{2g}^4, e_g^2\right)$ and there is considerable orbital angular momentum contribution to the overall magnetic moment of the compound. The observed long-range antiferromagnetic ordering in **1** could occur via the super exchange coupling involving both the oxalate and phosphate groups. It should be noted that the oxalate in the bis-bidentate coordination mode has proven to be a very effective ligand to mediate strong magnetic interactions between paramagnetic centers [46]. Many 2D and 3D network structures constructed from such coordinated oxalates and paramagnetic centers can show strong, long-range magnetic interactions ranging from ferro- to ferri- to anti-ferromagnetic behavior [47]. Within the infinite 2D sheet $[Co(C_2O_4)]_n$ in **1** the strong super exchange interactions could occur. Additional super exchange coupling involving phosphates can act to extend such interactions into the third dimension. This notion is consistent with the experimentally observed magnetic behavior in the other metal phosphoxalate systems [10,13,15,16,19,20,31,32,34,35,38].

3.5. Thermal analysis

The TG/DTG curves of **1** showed that the compound is thermally stable up to 298 °C. Between 298 and 394 °C, there are three exothermic events accompanying roughly three-stage weight loss resulted from the oxidation of the organics (see Fig. 2 of the Supplementary Materials). No further weight loss was observed at temperature higher than 496 °C. The total weight loss in this temperature range is ca. 41.8%, which agrees well with the expected weight loss of 40.44% for the collapse of the open-framework structure and formation of sodium cobalt phosphate. Heating the bulk material at 510 °C in air for 4 h showed that the bulk thermal decomposition product of **1** at this temperature gave a blue crystalline powder. The X-ray diffraction studies identified the product as the hexagonal phase of $NaCoPO_4$, one of the four known phases for this compound (see Fig. 3 of the Supplementary Materials).

4. Conclusions

We have demonstrated that the direct metathesis reaction can provide a viable alternative for preparing open-framework phosphoxalate compounds. This synthetic strategy is currently employed in our lab to explore the synthesis of a potentially large number of new inclusion compounds with interesting chemical and physical properties.

5. Supplementary materials

The experimentally observed and simulated X-ray powder diffraction pattern and TG/DTG Curves for **1** are provided as supplementary materials. Crystallographic data (excluding structure factors) for **1** have been deposited with the Cambridge Crystallographic Data Centre, CCDC__633399. The data can be obtained free of charge from the *Cambridge Crystallographic Data Centre* via www.ccdc.cam.ac.uk/data_request/cif.

Acknowledgments

We thank the National Science Foundation for financial support through a CAREER award to SDH (DMR-9733275). This work is partially supported by an OBR Research Challenge Grant through the Kent State University. We thank Ms. J. Gorka and Dr. M. Jaroniec for their help with the TGA experiments.

Appendix A. Supplementary materials

Supplementary data associated with this article can be found in the online version at doi:10.1016/j.jssc.2007.05.006

References

[1] R. Murugavel, M.G. Walawalkar, M. Dan, H.W. Roesky, C.N.R. Rao, Acc. Chem. Res. 763 (2004).
[2] R.C. Finn, R.C. Haushalter, J. Zubieta, Prog. Inorg. Chem. 51 (2003) 421.
[3] J.H. Yu, R.R. Xu, Acc. Chem. Res. 481 (2003).
[4] P. Amoros, M.D. Marcos, A. Beltran-Porter, D. Beltran-Porter, Curr. Opin. Solid State Mater. Sci. 4 (1999) 123.
[5] A.K. Cheetham, G. Ferey, T. Loiseau, Angew. Chem. Int. Ed. 38 (1999) 3268.
[6] P. Lightfoot, Z. Lethbridge, R. Morris, D. Wragg, P. Wright, A. Kvick, G. Vaughan, J. Solid State Chem. 143 (1999) 74.
[7] K. Kedarnath, A. Choudhury, S. Natarajan, J. Solid State Chem. 150 (2000) 324.
[8] N. Rajic, N.Z. Logar, G. Mali, V. Kaucic, Chem. Mater. 15 (2003) 1734.
[9] L. Peng, J. Li, J. Yu, G. Li, Q. Fang, R. Xu, J. Solid State Chem. 178 (2005) 2686.
[10] A. Choudhury, S. Natarajan, Solid State Sci. 2 (2000) 365.
[11] H. Lin, K. Lii, Y. Jiang, S. Wang, Chem. Mater. 11 (1999) 519.
[12] A. Choudhury, S. Natarajan, C.N.R. Rao, Chem. Mater. 11 (1999) 2316.
[13] A. Choudhury, S. Natarajan, J. Mater. Chem. 9 (1999) 3113.
[14] Z. Lethbridge, P. Lightfoot, J. Solid State Chem. 143 (1999) 58.
[15] A. Choudhury, S. Natarajan, C.N.R. Rao, J. Solid State Chem. 146 (1999) 538.
[16] A. Choudhury, S. Natarajan, C.N.R. Rao, Chem. Eur. 6 (2000) 1168.
[17] W. Chang, H. Lin, K. Lii, J. Solid State Chem. 157 (2001) 233.
[18] N. Rajic, D. Stojakovic, D. Hanzel, N.Z. Logar, V. Kaucic, Microporous Mesoporous Mater. 55 (2002) 313.
[19] Y. Jiang, S. Wang, K. Lii, Chem. Mater. 15 (2003) 1633.
[20] Y. Jiang, S. Wang, S. Lee, K. Lii, Inorg. Chem. 42 (2003) 6154.
[21] H. Meng, G. Li, Y. Xing, Y. Yang, Y. Cui, L. Liu, H. Ding, W. Pang, Polyhedron 23 (2004) 2357.
[22] C. Chen, P. Chu, K. Lii, Chem. Commun. 1473 (1999).
[23] L. Hung, H. Kao, K. Lii, Chem. Mater. 12 (2000) 2411.
[24] K. Lii, C. Chen, Inorg. Chem. 39 (2000) 3374.
[25] C. Choi, F. Anokhina, C. Day, Y. Zhao, F. Taulelle, C. Huguenard, Z. Gan, A. Lachgar, Chem. Mater. 14 (2002) 4096.
[26] M. Mrak, U. Kolitsch, C. Lengauer, V. Kaucic, E. Tillmanns, Inorg. Chem. 42 (2003) 598.
[27] T. Loiseau, G. Ferey, M. Haouas, F. Taulelle, Chem. Mater. 16 (2004) 5318.
[28] Z. Chen, S. Tan, L. Weng, Y. Zhou, X. Gao, D. Zhao, J. Solid State Chem. 179 (2006) 1931.
[29] Y. Huang, K. Lii, J. Chem. Soc. Dalton Trans. 4085 (1998).
[30] Z. Chen, L. Weng, J. Chen, M. Chen, D. Zhao, Stud. Surf. Sci. Catal. 154 (2004) 1118.
[31] Z.A.D. Lethbridge, A.D. Hillier, R. Cywinski, P. Lightfoot, J. Chem. Soc., Dalton Trans. 1595 (2000).
[32] Z.A.D. Lethbridge, S. Tiwary, A. Harrison, P. Lightfoot, J. Chem. Soc., Dalton Trans. 1904 (2001).
[33] Y. Jiang, S. Wang, S. Lee, K. Lii, Inorg. Chem. 42 (2003) 6154.
[34] Z.A.D. Lethbridge, M.J. Smith, S.K. Tiwary, A. Harrison, P. Lightfoot, Inorg. Chem. 43 (2004) 11.
[35] R. Yu, X. Xing, T. Saito, M. Azuma, M. Takano, D. Wang, Y. Chen, N. Kumada, N. Kinomura, Solid State Sci. 7 (2005) 221.
[36] M. Lee, S. Wang, Chem. Mater. 11 (1999) 3588.
[37] S. Natarajan, J. Solid State Chem. 139 (1998) 200.
[38] Y. Tsai, S. Wang, C. Huang, K. Lii, Inorg. Chem. 38 (1999) 4183.
[39] J. Do, R.P. Bontchev, A.J. Jacobson, Inorg. Chem. 39 (2000) 3230.
[40] J. Do, R.P. Bontchev, A.J. Jacobson, Chem. Mater. 13 (2001) 2601.
[41] M. Tang, K. Lii, J. Solid State Chem. 177 (2004) 1912.
[42] S. Neeraj, S. Natarajan, C.N.R. Rao, J. Chem. Soc., Dalton Trans. 289 (2001).
[43] Y. Zhong, Y. Sun, G. Yang, Acta Crystallogr. C 60 (2004) 504.
[44] teXsan Crystal Structure Analysis Package, Molecular Structure Corporation, 1992.
[45] J.S. Chen, R.H. Jones, S. Natarajan, M.B. Hursthouse, J.M. Thomas, Angew. Chem. Int. Ed. 33 (1994) 639.
[46] O. Kahn, Molecular Magnets, VCH, Weinheim, Germany, 1993.
[47] M. Pilkington, M. Gross, P. Franz, M. Biner, S. Decurtins, H. Stoeckli-Evans, A. Neels, J. Solid State Chem. 159 (2001) 262.